

# Electrospinning Nanofibres Of Pullulan Extracted From Phylloplane Fungus, *Aureobasidium Pullulans*

Komal Saraf (✉ [komal.saraf@gmail.com](mailto:komal.saraf@gmail.com))

Central Institute for Research on Cotton Technology <https://orcid.org/0000-0003-1156-3477>

N Vigneshwaran

Principal Scientist, ICAR -Central Institute of Research on Cotton Technology, Mumbai 400019, India


---

## Research

**Keywords:** Aureobasidium pullulans, BET surface area, Electrospinning, Nanofibres, NMR, Pullulan

**Posted Date:** September 18th, 2020

**DOI:** <https://doi.org/10.21203/rs.3.rs-70718/v2>

**License:**  This work is licensed under a Creative Commons Attribution 4.0 International License. [Read Full License](#)

---

## Abstract

*Aureobasidium pullulans* isolated from the phylloplane of *Peltophorum* tree, produced pullulan, an extracellular polysaccharide. It was grown on three different carbon sources, sucrose, wheat bran and cotton stalk dust, for maximizing the pullulan yield. *A. pullulans* (67.4 gL<sup>-1</sup>) had the highest yield followed by *A. pullulans* MTCC 1991 (63.68 gL<sup>-1</sup>). Pullulan was characterized by X-ray diffractometer (XRD), Brunauer-Emmett-Teller (BET) surface area analyzer, DSC and NMR. Electrospinning of pullulan blended with poly (vinyl alcohol) (PVA) produced bead-less nanofibres. The optimized parameters for electrospinning were 25 kV applied voltage, 0.5 mL/h flow rate, 18% polymer concentration (pullulan + PVA) and 150 mm tip-to-collector distance. The pullulan nanofibre was characterized by SEM, AFM, BET, contact angle measurement, DSC and CIE color space analyzer. A maximum surface area of 183.4 m<sup>2</sup>/g while the minimum nanofibre diameter (79 ± 19 nm by SEM) was obtained for the electrospun mat of commercial pullulan + 40% PVA. This work signifies the importance of pullulan extracted from an isolate of *Peltophorum* tree for conversion to high surface area nanofibres by electrospinning process.

## Introduction

Pullulan (poly-  $\alpha$ -1, 6-maltotriose) is a unique neutral water-soluble exopolysaccharide (EPS) produced in large quantities by microbial fermentation, mostly by *Aureobasidium pullulans*. Though sucrose and starch are traditional carbon sources, low-cost agricultural wastes like cassava starch residue, wheat bran and rice bran were also being evaluated for pullulan production to make it more economical as against petroleum-derived polymers (Ray et al. 2007). Pullulan is a promising biopolymer having a wide range of commercial and industrial applications in many fields like food science, health care, pharmacy and even in lithography (Singh et al. 2008). Other applications include bio-composite films, oxygen-impermeable coatings, adhesives, plywood, medicine and as fibre (Singh et al. 2008; Leathers et al. 2003; Knapp et al. 2010; Kong et al. 2014). For these special uses, polymer purity and molecular weight are important properties (Pollock et al. 1992; Punnapayak et al. 2003). So, research is also focused on developing an *A. pullulans* strain with enhanced pullulan productivity and raw material utilization ratio using a new method for genome shuffling of *A. pullulans* N3.387 (Kang et al. 2011).

*A. pullulans* is a yeast-like Ascomycete of Dothideales Order and Saccoteciaceae Family. They produce poly ( $\beta$ -L-malic acid), heavy oil liamocins, siderophore, and aubasidan-like  $\beta$ -glucan along with pullulan (Prasongsuk et al. 2018). *A. pullulans* var. *pullulans*, *A. pullulans* var. *melanogenicum*, and *A. pullulans* var. *aubasidani* are its three varieties based on the differences in its morphological and biochemical properties (Urzi et al. 1999; Yurlova et al. 1996; Zalar et al. 2008). The variety *A. pullulans* var. *melanogenicum* differs from the other varieties for its melanin production which occurs in the initial stages of growth and changes the colour of the colonies i.e. olive green to black color. The variety *A. pullulans* var. *aubasidani* shows negative response to the assimilation of methyl- $\alpha$ -D-glucoside and lactose and this feature is specific to this variety differentiating it from the other varieties (Yurlova et al. 1996). This strain produces aubasidan-like Pullulan (glucans with  $\alpha$ -1, 4-D-,  $\beta$ -1, 6-D- and  $\beta$ -1, 3-D-glycosidic bonds) (Yurlova et al. 1999).

A large variety of plants belonging to temperate, tropical and mediterranean regions have been known to colonize basidiomycetous and ascomycetous yeasts in their phylloplane (Glushakova et al. 2010; SlÁviková et al. 2009; Landell et al. 2010). The commonly found yeasts in the phylloplane were basidiomycetes such as *Cryptococcus laurentii*, *Rhodotorula mucilaginosa*, *Rhodotorula glutinis* and *Sporobolomyces roseus* (Sharma et al. 2009). *Debaryomyces hansenii*, *Hanseniaspora uvarum*, *Kazachstania barnetii*, *Metschnikowia pulcherima*, *Metschnikowia reukaufii*, *Pichia membranifaciens*, *Saccharomyces cerevisiae* and various species of *Candida* were some of the ascomycetous species found in the phylloplane (Koowadjanakul et al. 2011). Limtong et al. (2012) have tested the external surface of plant leaves, usually referred as phylloplane, for the growth of yeast and fungi known to produce pullulan. Youssef et al. (1998) have shown in their study that sucrose and olive oil when used as carbon sources can enhance the production of pullulan by *A. pullulans*. Kim et al. (2000) have used glucosamine as a carbon source in order to produce high molecular weight pullulan by *A. pullulans*.

As far as the environment is concerned, *A. pullulans* strains are dependent on dead and decaying matter, found mainly on the phylloplane in temperate areas (Punnapayak et al. 2003; Koowadjanakul et al. 2011). They help in keeping the environment clean with constant decomposition of organic material through the production of various enzymes that can breakdown cellulose, pectin, lignin and other plant wastes. This fungus has been isolated from rocks and monuments of moist and temperate conditions leading to blackening of rocks (Urzi et al. 1999). Although its omnivorous appetite is impressive, *A. pullulans* is a very adaptive fungus and of special interest because of its ability to produce an exopolysaccharide pullulan and many industrial enzymes like amylases, xylanases, pectinases etc.

Most of these strains were isolated from leaves of tropical plants. By in vitro digestibility study, it was reported that pullulan is less than 10% digestible and hence could act physiologically as dietary fiber or residue (Kunkel et al. 1994).

Currently, the cost of pullulan is comparatively higher than the petroleum based polymers and hence, their use is limited. To enhance their use, apart from the attempts to reduce their production cost, newer methods of usage need to be explored. Electrospinning can be a good alternative method that produces continuous non-woven biopolymer nanofibres with diameters from micron to nano scale range when an external electric field is imposed on a spinneret containing the biopolymer solution (Liu et al. 2013). Thus produced nanofibres find potential applications in wound dressing, scaffold for tissue engineering, biosensors, drug delivery, gas barrier films and nanocomposites. Since the beginning of the 21<sup>st</sup> century, electrospun nanofibres have been widely studied and a wide range of applications have been made, such as in energy storage, healthcare, environmental engineering, defense and security (Eslamian et al. 2019). Hence, this work explores the possibility of using cheaper carbon source for pullulan production and their electrospinning potential for production of nanofibre mat and their characterization.

## Materials And Methods

### Fungal strains and culture media

Isolation of pullulan producing fungi was carried out in a minimal salts medium (P2). Medium P2 included (per liter of deionized water): 1 g of  $(\text{NH}_4)_2\text{HPO}_4$ ; 0.5 g of NaCl; 0.05 g of  $\text{MgSO}_4 \cdot 7\text{H}_2\text{O}$ ; 2 g of  $\text{K}_2\text{HPO}_4$ ; 0.01 g each of  $\text{FeSO}_4$ ,  $\text{MnSO}_4$ , and  $\text{ZnSO}_4$ ; and HCl to pH 7.0. Sucrose was added to 1% (w/v). Agar was included at  $15 \text{ gL}^{-1}$  for solid plates.

*A. pullulans* MTCC 1991 was obtained from the culture collection of IMTECH Chandigarh, India. P2 medium with 5% sucrose was used to carry out submerged fermentation (SF). Wheat Bran (WB) and Cotton Stalk Dust (CSD) were obtained from the local market in Mumbai, India and used as solid substrate and sole carbon source for Solid State Fermentation (SSF). A basal production medium for SSF was prepared as follows: 3.5 g of sodium glutamate; 5 g of  $\text{K}_2\text{HPO}_4$ ; 2 g of  $\text{KH}_2\text{PO}_4$ , 2g of  $\text{MgSO}_4$ ; 1g of NaCl and 0.5g of  $\text{FeSO}_4 \cdot 7\text{H}_2\text{O}$  per liter and pH adjusted to 6.5 with 1N HCl. Solid substrate was prepared by taking 20 g of substrates in 250 mL Erlenmeyer flasks and amended with 40 mL of basal medium (1:2 ratio, w/v) and thoroughly mixed. The prepared solid substrate was sterilized in an autoclave at 121 °C for 20 min and cooled to ambient temperature. All the chemicals used to make media were of analytical grade.

### Isolation of pullulan producing fungi by selective enrichment

Leaves (old and young) were removed from *Peltophorum* tree and soaked in sterile water for 3 days at 25 °C, and then 0.1 mL of soaked water was transferred to 10 mL of P2 minimal salts medium (pH 4) containing 1% (w/v) sucrose and 10 µg/mL of chloramphenicol. After 2 days of shaking of P2 medium broth at 25 °C, the turbid culture was allowed to stand undisturbed for 20 min to allow filaments and aggregates to settle to the bottom. About 10 µL, from the upper partially clarified phase that, was enriched for yeast-like cells were spread onto agar plates containing P2 medium (pH 5), 1% (w/v) sucrose and 10 µg/mL of chloramphenicol. After 4 days, independent colonies were purified by sub-culturing.

### Pullulan production

The fungal inoculums of *A. pullulans* MTCC 1991 and the isolates were prepared as follows. A loop full of each culture was inoculated in basal medium and incubated at 30 °C for 48 h. About 0.5 mL culture was added to 40 mL of P2 (5% sucrose) liquid medium and the cultures were shaken at 200 rpm at 25 °C for 66 h for SF. While for SSF, 2 mL of 48 h old cultures grown on basal medium was inoculated in 20 g of solid substrates with 40 mL basal medium and incubated at 30 °C for 7 days. All the samples were analyzed in triplicates and the yields were expressed as average ± standard deviation (S.D.).

### Biochemical Analysis of the substrates used for SSF

To determine the biochemical composition of WB and CSD, moisture content was determined by drying in hot air oven at 105 °C for 5 h, protein estimation (total nitrogen x 5.7 for WB and 6.25 for CSD) was determined by Kjeldahl method using Kelplus<sup>®</sup> Instrument (Pelican Equipments, Chennai, India) and ash content was determined by heating in a muffle furnace at  $550 \pm 25$  °C for 3 h. Crude fibre was determined by Weende's method of acid and alkali digestion using Fibraplus<sup>®</sup> Instrument (Pelican Equipments, Chennai, India). All the parameters were analyzed in triplicates and were expressed as average ± (S.D.).

### Downstream processing for extraction of EPS

The samples of SF, where 5% sucrose as carbon source was diluted with 1 volume of deionized water and centrifuged, and the EPS were recovered from the clarified broth by precipitation with 1 volume of Isopropyl alcohol (IPA). The precipitate was removed and dried to constant weight in an oven at 80 °C. In case of SSF, the fermented mass was washed thoroughly with 5 volumes of deionized water by shaking at 250 rpm for 2 h. Cheese cloth was used for coarse filtration and centrifugation at 5488 x g for 45 min at 4 °C for finer particles separation. Pullulan was precipitated using 2 volumes of IPA after addition of 2% KCl in the aqueous extracts. The precipitated pullulan was collected on pre-weighed weighing bottle and dried at 80 °C till constant weight. The yield of pullulan was expressed as gL<sup>-1</sup> of production medium in SF and as gL<sup>-1</sup> of basal medium in SSF.

### Screening of isolates for pullulan production

The extracted EPS from the isolates were tested for the presence of pullulan on the basis of the set of identification tests like solubility in water, pH of 10% solution in the range of 5-7, white precipitate formation with Polyethylene glycol 600 (PEG 600) and functional group analysis by Fourier transform infrared (FT-IR) (IR Prestige 21<sup>®</sup> model) by KBr pellet method. For PEG 600 test, 2 mL of PEG 600 was added to 10 mL of 2% aqueous EPS solution, development of white precipitate indicated a positive test for pullulan. FT-IR spectra were recorded with the following parameters: 64 scans; resolution, 4 cm<sup>-1</sup> over the KBr pellet. Pullulan sample (1 mg) was manually well blended with 100 mg of KBr powder. These mixtures were then desiccated overnight at 50°C under reduced pressure prior to FTIR measurement. The pullulan extracted from *A. pullulans* MTCC 1991 and commercial pullulan were used for comparison. The cultures, that gave positive results for the above mentioned tests, were processed further for morphological and biochemical analysis for identification.

### Morphological and biochemical analysis for identification

Identification of the cultures and assessment of nutritional physiology were carried out as per the identification key provided in the literature (Yurlova et al. 1996; Yurlova et al. 1999). Morphology of the colonies was studied on different culture media: Potato Dextrose Agar (PDA, Himedia), Blakeslee's Malt Extract Agar (MEA) and Yeast Morphology Agar (YMA, Himedia) and incubated at 30 °C for 7–14 days in darkness. Morphological characteristics of the isolated fungal cells were studied under light microscopy in slide culture on PDA at 30 °C for 7 days. Wet mount of the cultures were performed to determine the structure of hyphae and conidiophore. The fungal isolate was also sent to National Fungal Culture Collection of India (NFCCI)-A National Facility, Agharkar Research Institute, Pune, India for morphological characterization. Assimilation tests of carbon and nitrogen compounds were tested in liquid media of Yeast Nitrogen Base (YNB) and Yeast Carbon Base (YCB) respectively at 30 °C up to 14 days. The stock solutions were sterilized by filtration and refrigerated until further use. Carbon sources used are 2% each of D-Xylose, D-Arabinose, Ethanol, D (+) Melibiose, α methyl-D-glucoside and D-Lactose whereas nitrogen source tested is D-glucosamine (Yurlova et al. 1996; Kurtzman et al. 2011). Urease production was tested in Christensen's Urea Broth and incubate at 37 °C for 48 h. Citrate utilization was studied using Simmon Citrate Agar (Himedia<sup>®</sup>) incubated at 30 °C for 7 days. Growth at 37 °C was tested in Malt Extract Broth incubated for 7 days. Solubilization of CaCO<sub>3</sub> was performed in CaCO<sub>3</sub> agar medium (Himedia<sup>®</sup>, India). The fungal isolate was sent to National Centre for Microbial Resource (NCMR), NCCS, Pune for sequencing and deposition.

### Characterization of pullulan

Extracted pullulan was subjected to X-ray diffractometer (XRD, X'pert Pro, PANalytical<sup>®</sup>) to study the crystallinity. Wide angle X-ray diffraction patterns were obtained with nickel filtered Cu Kα (λ = 1.54 Å) radiation and analyzed using automatic powder diffraction (APD) software. The diffracted intensities were recorded from 5° to 80° 2θ angles. The crystallite height (I<sub>002</sub>), measured at the peak around 20° 2θ angle, and amorphous height (I<sub>am</sub>), measured at the valley around 11° 2θ angle, were used to calculate the apparent crystallinity index (apparent Cr.I.) using the empirical method (Choudhury et al. 2013) as per the equation (1).

$$\text{Cr.I} = \left( \frac{1002 - I_{\text{am}}}{1002} \right) * 100 \quad \dots (1)$$

The average pore size, total pore volume and specific surface area were determined by Brunauer-Emmett-Teller (BET) method. Samples were degassed at 160 °C for 3.5 h under vacuum before analysis. BET analyses were performed using Quantachrome Nova model and Novawin software and using the equation (2).

$$\frac{1}{\left[ V a \left( \frac{P_o}{P} - 1 \right) \right]} = C - \frac{1}{V m C} \times \frac{P}{P_o} + \frac{1}{V m C} \quad \dots (2)$$

Where, P = partial vapor pressure of adsorbate gas in equilibrium with the surface at 77.4 K (boiling point of liquid nitrogen), in Pascals; P<sub>o</sub> = saturated pressure of adsorbate gas, in Pascals; V<sub>a</sub> = volume of gas adsorbed at standard temperature and pressure (STP) [273.15 K and atmospheric pressure (1.013 × 10<sup>5</sup> Pa)], in mL; V<sub>m</sub> = volume of gas adsorbed at STP to produce an apparent monolayer on the sample surface, in mL; C = dimensionless constant that is related to the enthalpy of adsorption of the adsorbate gas on the powder sample. A value of V<sub>a</sub> is measured at each of not less than 3 values of P/P<sub>o</sub>. Then the BET value calculated as given in equation (2) is plotted against P/P<sub>o</sub> according to the equation (3). This plot should yield a straight line usually in the approximate relative pressure range 0.05 to 0.3. All the parameters were analyzed in triplicates and were expressed as average ± standard deviation (S.D.).

$$\frac{1}{V a \left( \frac{P_o}{P} - 1 \right)} \quad \dots (3)$$

The thermal properties of the extracted pullulan were evaluated by a differential scanning calorimeter (Mettler Toledo TC-15 TA). Samples were placed onto aluminum crucibles and then the runs were carried out from room temperature to 450 °C at a heating rate of 10 °C min<sup>-1</sup> under nitrogen atmosphere.

For <sup>1</sup>H-NMR spectroscopy, the solutions were prepared by dissolving 5 to 9 mg of commercial as well as lyophilized pullulan samples per mL of D<sub>2</sub>O (Sigma Aldrich, USA) and analyzed using Agilent 600 MHz AR Spectrophotometer, USA. The raw data was processed using the Vnmrj<sup>®</sup> software.

### Electrospinning of pullulan

The extracted pullulan from *A. pullulans* MTCC 1991 and *A. pullulans* were dissolved in distilled water with the help of heating and magnetic stirring. Final concentration was adjusted to 18% for extracted pullulan and 12% for commercial pullulan for electrospinning. For the electrospinning solution, pH was measured by pH meter (El Model – 1012E), particle size and zeta potential by using Zeta Sizer Nicomp<sup>™</sup> 380 ZLS (Santa Barbara, California, USA), conductivity by using Conductivity meter (Eutech Instruments, Con 2700) and viscosity by Brookfield DV III Ultra Programmable Rheometer. All the parameters were analyzed in triplicates and were expressed as average ± S.D. The electrospinning was carried out with varying proportions PVA and pullulan for bead-less nanofibre formation. The in-house assembled electrospinning system consisted of a fume hood housing the equipment, syringe pump (New Era Pump Systems, Inc.) with a syringe having a metallic needle, a controllable high-voltage source (0 to 50 kV) connected to the needle, and a grounded copper foil wrapped collector plate for collection of the fibrous mats. Optimization experiments were carried out by varying the following process conditions: 15-20 cm tip to collector distance (TCD); 0.2 to 1.0 mL/h flow rate; and 15 to 25 kV voltages to obtain the bead-less nanofibres.

### Characterization of pullulan nanofibre mats

The morphology of electrospun nanofibres was studied using a scanning electron microscope (SEM), Philips XL-30, with an accelerating voltage of 12 kV. Each sample was coated with a thin layer of conducting material (gold/palladium) using a sputter coater before SEM analysis. The SEM images were analyzed in Image J<sup>®</sup> software to determine the average diameter of nanofibres. The morphology of nanofibres was observed and fibre diameter, roughness and surface area were measured using Atomic Force Microscope (AFM), (diInnova<sup>®</sup> SPM Veeco, Santa Barbara, CA, US), equipped with a 90 μm scanner by tapping mode in ambient condition. The silicon nitride cantilever with a spring constant of 40 Nm<sup>-1</sup> was used for scanning. The scan rate of 1.0 Hz and 512 lines per 10 μm were used to optimum contrast. No filtering was done during scanning. The average pore size, total pore volume and specific surface area were determined by BET analyzer. Samples were degassed at 160 °C for 3.5 h under vacuum before analysis. All the parameters were analyzed in triplicates and were expressed as average ± standard S.D.

Water contact angle was measured using GBX ILMS Version 3.6 instrument to study the hydrophilic nature of the electrospun nanofibre mats. Using a microsyringe, 5 μL deionized water was dropped perpendicularly to each surface of the mat placed on a horizontal glass sheet. Then, the images of water drops on the surface of the mat were recorded and analyzed. The thermal properties of the nanofibre

mats were evaluated by a differential scanning calorimeter (Mettler Toledo TC-15 TA®). Samples were cut into small pieces and placed onto aluminum crucibles and then the runs were carried out from room temperature to 450 °C at a heating rate of 10 °C min<sup>-1</sup> under nitrogen atmosphere. For determining the grey values of developed electrospun nanofibre mats, the CIE (International Commission of Illumination) color space coordinates were determined. A color is defined by its RGB values which give the amount of red, green and blue in a particular color. In CIE L\*a\*b\* color space values, L\* stands for lightness, a\* and b\* for the green–red and blue–yellow color components and ΔL represents brightness difference between samples. The magnitude of color difference was quantified as ΔE.

## Results And Discussion

### Isolation of pullulan producing fungi by selective enrichment

Selective enrichment of the extract from *Peltophorum* leaves resulted in five isolates namely OL1, OL2, OL3 obtained from old leaf and YL1 and YL2 obtained from young leaf respectively.

### Discussion:

All isolates were maintained on P2 as well as PDA media. P2 medium was used as it contained minimal salts medium plus sucrose and low pH, which acted as basis for selective enrichment. Chloramphenicol was added to prevent bacterial growth during enrichment and isolation. After incubation for 2 days at 30 °C, the color of the colony ranged from off-white or light beige to pale pink to green and black appeared.

### Production of pullulan and screening of isolates for pullulan production

The five isolates were subjected to screening for pullulan production by SF and SSF. Basal medium consisting of trace elements, mineral nutrients and buffering agents was used to supplement the solid substrate for pullulan production. Pullulan yield was higher for WB by SSF as compared to 5% Sucrose in SF. CSD could not be utilized to produce pullulan, as the precipitates extracted from the cultures post fermentation were insoluble in water which is a preliminary confirmatory qualitative test for identification of pullulan (Table 1).

**Table 1 EPS from *A. pullulans* MTCC 1991 and isolates using different carbon sources and qualitative tests for identification of pullulan**

Sr. No.	Culture / Sample details	EPS yield (gL <sup>-1</sup> ± SD)			Solubility in water	Precipitate with PEG 600	pH
		Sucrose (SF)	WB (SSF)	CSD (SSF)			
1	<i>A. pullulans</i> MTCC 1991	1.83 ± 0.15	63.68 ± 2	15.15 ± 0.25	+	+	6.5
2	OL1	2.28 ± 0.2	28.70 ± 0.66	12.90 ± 0.14	-	NA	NA
3	OL2	1.93 ± 0.19	44.43 ± 1.5	10.08 ± 0.16	-	NA	NA
4	OL3	0.55 ± 0.22	67.4 ± 2.2	11.73 ± 0.2	+	+	5
5	YL1	0.69 ± 0.28	30.2 ± 0.85	14.08 ± 0.23	-	NA	NA
6	YL2	0.6 ± 0.21	35.25	9.45 ± 0.1	-	NA	NA
7	Commercial pullulan	NA	NA	NA	+	+	5.5

**Table 2 Biochemical Analysis of the substrates used for SSF**

Sr. No.	Constituents	Average	Average
		WB (%) $\pm$ SD	CSD (%) $\pm$ SD
1	Moisture	8.08 $\pm$ 0.55	9.58 $\pm$ 2.2
2	Crude fibre	10.25 $\pm$ 2	30.91 $\pm$ 4.5
3	Nitrogen	3.85 $\pm$ 0.63	1.5 $\pm$ 0.17
4	Crude Protein	21.9 $\pm$ 3.6	9.37 $\pm$ 1.1
5	Total Ash	5.5 $\pm$ 0.76	10.93 $\pm$ 3.3

As per the results in Table 1, various cultures including *A. pullulans* MTCC 1991 as well as isolates were screened for the production of pullulan. The yield obtained for *A. pullulans* MTCC 1991 using WB in SSF was found to be 63.68 gL<sup>-1</sup>. Also the isolate, OL3 gave a yield of 67.4 gL<sup>-1</sup> using WB in SSF. As seen in Fig. 1, the FTIR spectra showed strong absorption at around 3400 cm<sup>-1</sup> indicated that all the pullulan had some repeating units of -OH as in sugars. The other strong absorption at 2926 cm<sup>-1</sup> indicated a SP3-hybridisation of C-H bond, around 1600 cm<sup>-1</sup> for the O-C-O bond, around 1300 cm<sup>-1</sup> for C-O-H bond, 1000 cm<sup>-1</sup> for the C-O bonds in the alkane compounds existed in all the samples. **Fig. 1** FTIR spectra of Commercial Pullulan (**a**), Pullulan of *A. pullulans* MTCC 1991 (**b**) and EPS of OL3 (**c**)

### Discussion:

SSF has gained importance recently due to several advantages over SF such as lower investment, easy operation and simplified downstream processing. Two undesirable features of SF of *A. pullulans* are reported. The decrease in culture viscosity during submerged growth resulted in decrease of average molecular weight of the accumulated extracellular pullulan from 3 x 10<sup>6</sup> - 6 x 10<sup>6</sup> to 1 x 10<sup>5</sup> - 2 x 10<sup>5</sup> Da. Also, there is a simultaneous synthesis of dark melanin-like pigment, which contaminates the pullulan (Pollock et al. 1992b; Punnapayak et al. 2003).

As per the results in Table 1, the yield obtained for *A. pullulans* MTCC 1991 using WB in SSF was more than the reported commercial production rate (25 to 61 gL<sup>-1</sup>) in liquid medium (SF) (Pollock et al. 1992; Choudhury et al. 2013; Karim et al. 2011). Earlier research reported the use of jackfruit seed powder based medium components for pullulan production by *Aureobasidium pullulans* and the maximum pullulan concentration of 17.95 (gL<sup>-1</sup>) only was produced in the validation experiment (Sharmila et al. 2013). Also the isolate, OL3 gave more yield than *A. pullulans* MTCC 1991 using WB in SSF. Thus, WB could be a promising economic substrate for production of pullulan in SSF. Thus the above results support the finding that WB has more than 50% nutritional value (Table 2) as compared to CSD, making it a good solid substrate for pullulan production by SSF. Pullulan content and color depends on the strain of microorganisms used and the chemical composition of the substrate. Earlier work reported the preference of glucose over sucrose for production of pullulans by *A. pullulans* (Punnapayak et al. 2003).

As seen in Fig. 1, the FTIR spectrum of the commercial grade pullulan matches well with the EPS produced by *A. pullulans* MTCC 1991 and the isolate, thereby confirming the production of pullulan.

### Morphological and biochemical analysis for identification

The selected fungal isolate for pullulan production, OL3 was subjected to identification based on morphological and nutritional physiological characteristics. Fungal growth in standard conditions (PDA at 30 °C) occurred within 48 h that were not pigmented or light pink at the beginning, later became olive green-black. As per Fig. 2, *A. pullulans* MTCC 1991 and OL3 had septate hyphae of diameter more than 2  $\mu$ m. The conidiophore bearing conidia were observed for *A. pullulans* MTCC 1991 and prototunicate asci and blastic conidiogenesis of OL3 were also observed. Growth on different cultural media (PDA, MEA and YMA) affected both the morphology and pigment production. Variation in colony color was also detected when the fungi were cultivated on MEA for seven days.

Following the identification keys provided earlier (de Hoog et al. 1994) and morphological appearance, the isolate namely OL3 was identified as *Aureobasidium pullulans* (de Bary & Lowenthal) G. Arnaud. This has also been confirmed by the morphological characterization carried out by National Fungal Culture Collection of India (NFCCI)-A National Facility, Agharkar Research Institute, Pune,

India. As per the sequencing results done by Internal transcribed spacer (ITS) method, it was found that the strain showed 99% similarity with *Aureobasidium melanogenum* CBS 105.22, carried out at NCMR-NCCS, Pune, India. The same strain has been deposited at NCCS, Pune, with the accession number MCC 1868.

**Table 3 The nutritional physiology profiles of *A. pullulans* MTCC 1991 and isolate OL3**

Characteristics	<i>A. pullulans</i> MTCC 1991	Isolate OL3
<b>Carbon sources</b>		
D - Xylose	+	+
D - Arabinose	+	+
Ethanol	+	+
D (+) Melibiose	+	+
$\alpha$ methyl-D-glucoside	+	+
D-Lactose	+	+
<b>D-glucosamine</b>	+	+
<b>Citrate</b>	+	+
<b>Urea hydrolysis</b>	+	+
<b>Temperature tolerance</b>		
25 °C	+	+
30 °C	+	+
37 °C	-	-
<b>CaCO<sub>3</sub> Solubilization</b>	-	-

#### Discussion:

The nutritional physiology profiles of isolate OL3 corresponded well to those of *A. pullulans* MTCC 1991 as shown in Table 3. Cultures equivalent to identified strain of culture *Aureobasidium pullulans* (de Bary & Lowenthal) are NCIM 1048, ATCC 42023, DSM 3042, ATCC 62922.

#### Physical characterization of pullulan

The XRD patterns of pullulan extracted from *A. pullulans* MTCC 1991 and *A. pullulans* (Fig. 3) had a very distinct broad valley and peak, indicating the amorphous and crystalline nature of the material. The deepest point of the valley was considered for calculation purpose of amorphous region. The apparent crystallinity indices of commercial pullulan, *A. pullulans* MTCC 1991 and *A. pullulans* were calculated as 29.0%, 45.8% and 18.3%, respectively.

As seen in Table 4, the average pore radius of commercial pullulan and that of extracted pullulan from *A. pullulans* MTCC 1991 as well as isolates was the same around 24-30 Å. Similarly the total pore volume was found to be in the range 0.02 to 0.075 cc g<sup>-1</sup>.

**Table 4 BET analysis and solution properties of pullulans**



Sr. No.	Source of Pullulan	Average Pore Radius (Å) ± SD	Total Pore Volume (cc/g) ± SD	Surface area (m <sup>2</sup> /g) ± SD	pH	Mean diameter by DLS (nm) ± SD	Zeta potential (mV) ± SD	Viscosity (cP) ± SD	Conductivity (mS) ± SD
1	Commercial	24.34±0.04	0.02167±0.01	17.806±1.95	6.5±0.1	22.8±1.8	6.51 ± 0.35	74.6 ± 11	47.63 (μS)± 0.53
2	<i>A. pullulans</i> MTCC 1991	29.17±0.07	0.06847±0.005	46.949±1.4	7.6±0.12	697.9±21	28.04 ± 1.4	144 ±14	9.673 ±1.85
3	<i>A. pullulans</i>	29.59±0.08	0.06313±0.01	42.679±1.75	7.3±0.15	527.9±18	11.34 ± 0.75	265.2 ± 22	13.66 ± 2.5

As seen in the thermograms (Fig. 4),  $T_g$  values were 41, 43 and 43 for commercial pullulan, pullulans from *A. pullulans* MTCC 1991 pullulan and *A. pullulans* respectively. The range of melting temperature was found to be from 107 to 152 °C.

Structural characterization of pullulan was carried out by <sup>1</sup>H-NMR and <sup>13</sup>C-NMR spectroscopy and compared with that of commercial pullulan. Four chemical signals were displayed in the anomeric region between 4.4 to 5.3 ppm due to the four sugar repeating unit present in the pullulan polysaccharide. Signals were observed at 1.2 and 1.1 ppm was due to 6-deoxy-d-altrose present in the polysaccharide as shown in Fig. 5a. This confirms the presence of the major components of the pullulan structure in the extracted polymer as compared with the commercial in <sup>1</sup>H-NMR spectra. For all the extracted pullulans (Fig. 5b), it was found that there was splitting of C-6 (peaks between 60 to 62 ppm) and C-4 (peaks between 71 to 79 ppm) were due to C-1 of (1 → 4) linked glucose unit. C-6 signals arrived at around 60 ppm are due to two kinds of 1, 4 linked α-D glucose, whereas the signal at around 69 ppm corresponds to C-6 of the 1, 6 linked α-D glucose. There was a single peak between 82 and 88 ppm at around 84ppm which explained that very few of the sugar residues were available in furanose form and most of them were in pyranose form in biopolymer. Anomeric α (1 → 6) appeared by peak at around 99 ppm. Signals were detected in the 57.7–64.7 regions indicating that some C-6 positions were non-glycosylated. Anomeric α (1 → 6) was indicated by peak resonance at 99.73 ppm whereas anomeric α (1 → 4) was indicated by peak resonance at 100-101 ppm. None of the peaks were obtained between 93 and 97 ppm indicating the absence of oligomers.

## Discussion:

As per the results of XRD spectra, the apparent crystallinity indices of commercial pullulan, *A. pullulans* MTCC 1991 and *A. pullulans* match well with the literature reported values (Wu et al. 2013; Xiao et al. 2015). Although a highly crystalline polymer is stronger but it loses its flexibility since it is too brittle and cannot be reused as a plastic. The amorphous nature of the polymer gives it the ability to bend without breaking. It's important to know that fibres are always composed of polymers which are arranged into crystals showing regular arrangement (Zalar et al. 2008). Based on the above mentioned points, pullulan was found to be a balanced polymer.

The technique is named after its inventors; BET is the most frequent method for determination of specific surface area of porous materials. The measurement is based on physical adsorption of gas on the surface of the sample. As seen in Table 4, the average pore radii and total pore volume of the commercial pullulan and extracted samples were similar. But, the surface area for extracted pullulan was more than twice the surface area of commercial pullulan. It is also evident that particle size, charge, viscosity and conductivity, of the lyophilized pullulans from *A. pullulans* MTCC 1991 and *A. pullulans*, were significantly larger than commercial pullulan. The increased amount of charge as seen from the values of zeta potential corresponds to the increased conductivity of the extracted pullulans. This increased conductivity in turn would help in the process of electrospinning thereby giving larger surface area, pore size and pore volume.

The glass transition temperature ( $T_g$ ) was taken as the mid-point of the change of slope in the DSC curves. As per the literature depending on different sources of pullulan, the range of  $T_g$  of pullulan was from 38 to 59 °C (Xiao et al. 2015). As seen in the thermograms (Fig. 4),  $T_g$  values of the commercial and extracted samples matched well with the literature and also fall in the normal range. The change in melting point reflects the change in crystallinity of the polymer extracted from the cultures (Li et al. 2017).

Pullulan is a glucose polysaccharide of 20 kDa, consisting of maltotriose [ $\alpha$  (1,4) units attached by  $\alpha$ (1,6) linkages]. Hence the  $^{13}\text{C}$  spectrum should yield 18 resonances (Li et al. 2017; Arnosti et al. 1995). But, achieving all 18 peaks is difficult as there are chances for overlapping. All the peak resonances match well with the commercial pullulan and other references showing NMR spectra of pullulan except that there was absence of furanose form of sugar residues in them as seen in Fig. 5b (Ye et al. 2008; Sugumaran et al. 2014; Sugumaran et al. 2013). The additional peaks in the extracted pullulan might be due to the impurities present in the samples.

### Electrospinning of pullulan

The pH of the solution was found to be on the acidic side for commercial pullulan but neutral or slightly alkaline for the extracted pullulan. The zeta potential and conductivity of extracted pullulans were higher than that of commercial pullulan. The viscosity of extracted pullulans was higher than that of commercial pullulan. All the values are given in Table 4. Taking into account, pH, zeta potential, conductivity and particle size of the extracted pullulans, there was a need for a carrier polymer to aid the process of electrospinning to produce nanofibers for which PVA was chosen.

Throughout the experiment the applied voltage, flow rate, polymer concentration and TCD were fixed at 20kV, 0.5 mL h<sup>-1</sup>, 18% pullulan and 15 cm, respectively. The proportion of PVA required to produce nanofibres was found to be 50% for pullulan extracted from *A. pullulans* where as it was 40% for pullulan extracted from *A. pullulans* MTCC 1991. But, commercial pullulan gave beaded nanofibres with PVA (Fig. 6).

### Discussion:

Acidic solution tend to give better electrospinning due to presence of H<sup>+</sup> ion concentration aiding in attraction of polymer solution droplet from the tip of the collector towards the negative electrode when electric field is applied. So, the pullulan with neutral to alkaline pH was not getting electrospun without any carrier polymer. Higher zeta potential and conductivity let to increasing the charge carrying ability of the polymer jet which subjected to higher tension under the electric field, resulted in poor fibre formation. The viscosity range of different polymer solutions at which electrospinning is done is a major variable. Higher viscosity of extracted pullulans aided them to give continuous smooth fibres when electrospun whereas commercial pullulan having lower viscosity would give beaded fibres. PVA was used as a carrier polymer as it is relatively inexpensive, chemically and thermally stable, and not degradable under most physiological conditions. An earlier work reported the production of gelatin/polyurethane blended nanofiber by electrospinning having the potential application for use as a wound dressing, wherein the polyurethane was used to reduce the hydrophilicity of gelatin (Kim et al. 2009). Yet another work reported the production of a composite electrospun nanofibre using pullulan, PVA and montmorillonite clay having enhanced thermal stability and mechanical property (Islam et al. 2012).

The morphology of electrospun nanofibres can be affected by electrospinning instrument parameters including applied voltage, tip to collector distance (TCD), flow rate and solution parameters such as polymer concentration. Earlier work reported the electrospinning of chitosan from its solutions in 2% aqueous acetic acid by adding PVA as a "guest" polymer (Zhang et al. 2007).

### Characterization of nanofibre mats

The SEM images showed smooth bead free nanofibres for electrospun pullulan extracted from *A. pullulans* and *A. pullulans* MTCC 1991 but commercial pullulan gave beaded nanofibres (Fig. 6). As analyzed in Image J<sup>®</sup> software, the average diameter range of nanofibres was found to be 130 to 179 nm for commercial pullulan blended with PVA whereas the diameter range was 180 to 220 nm for pullulan extracted from *A. pullulans* and *A. pullulans* MTCC 1991 blended with PVA (see Table 5).

### Table 5 Size analysis of electrospun nanofibre mats of pullulan using SEM images

Sr. No.	Electrospun nanofibre mats	Diameter in nm (Average $\pm$ SD)
1.	Commercial pullulan	838 $\pm$ 53
2.	PVA	494 $\pm$ 74
3.	Commercial pullulan + 40 % PVA	179 $\pm$ 19
4.	Commercial pullulan + 50 % PVA	130 $\pm$ 23
5.	<i>A. pullulans</i> MTCC 1991 pullulan + 40% PVA	213 $\pm$ 78
6.	<i>A. pullulans</i> pullulan + 50% PVA	183 $\pm$ 33

The AFM images (Fig. 7) as analyzed in the SPM lab software showed that the fibres obtained on electrospinning of commercial pullulan and PVA were larger in height and diameter as compared to their blended fibres (Table 6). Also, the extracted pullulans blended with PVA not only gave thinner fibres than commercial polymer but also gave fibres in the nano-size range.

**Table 6 AFM analysis of pullulan / PVA nanofibres at 2 $\mu$ m magnification**

Sr. No.	Electrospun pullulan nanofibre mats	Average Height (nm) $\pm$ SD	Average Diameter (nm) $\pm$ SD	Average Roughness (nm) $\pm$ SD	Average Surface area ( $\mu$ m) <sup>2</sup> $\pm$ SD
1.	Commercial pullulan	145 $\pm$ 21	897 $\pm$ 42	14.2 $\pm$ 0.002	4.33 $\pm$ 1.6
2.	PVA	240 $\pm$ 35	1210 $\pm$ 78	35.5 $\pm$ 0.007	5.18 $\pm$ 0.4
3.	Commercial + 40% PVA	84 $\pm$ 14	413 $\pm$ 25	14.7 $\pm$ 0.0036	4.22 $\pm$ 2.1
4.	Commercial + 50% PVA	15.82 $\pm$ 3.5	128 $\pm$ 16	13.1 $\pm$ 0.0015	4.09 $\pm$ 1.2
5.	<i>A. pullulans</i> MTCC 1991 + 40% PVA	15.59 $\pm$ 4.2	260 $\pm$ 32	9.464 $\pm$ 0.0024	4.13 $\pm$ 2.7
6.	<i>A. pullulans</i> + 50% PVA	28.72 $\pm$ 8.8	383 $\pm$ 39	25.2 $\pm$ 0.009	4.07 $\pm$ 1.8

The BET analysis data measuring the average pore radius, total pore volume are given in the table 7. The average pore radius (8.664 Å) was smallest in case of the electrospun nanofibre mat produced from commercial pullulan + 40 % PVA. The total pore volume (0.08785 cc/g) was lowest in case of the electrospun nanofibre mat produced from *A. pullulans* pullulan + 50% PVA. The surface area (1302 m<sup>2</sup>/g) was the highest in case of the electrospun nanofibre mat produced from PVA alone. The surface area for commercial pullulan alone was found to be 183.4 m<sup>2</sup>/g. But the surface areas of their blended solutions were more than 183.4 m<sup>2</sup>/g, this is attributed to the high surface area of PVA nanofibres.

**Table 7 BET analysis of electrospun nanofibre mats of pullulan**

Sr. No.	Electrospun pullulan nanofibre mats	Average Pore Radius (Å) ± SD	Average Total Pore Volume (cc/g) ± SD	Average Surface area (m <sup>2</sup> /g) ± SD
1.	Commercial pullulan	15.20 ± 0.072	0.1394 ± 0.002	183.4 ± 5.7
2.	PVA	17.4 ± 0.085	1.133 ± 0.009	1302 ± 32
3.	Commercial + 40 % PVA	8.664 ± 0.041	0.1027 ± 0.0015	237 ± 11
4.	Commercial + 50 % PVA	18.08 ± 0.1	0.2003 ± 0.004	221.6 ± 9.5
5.	<i>A. pullulans</i> MTCC 1991 + 40% PVA	15.61 ± 0.079	0.1176 ± 0.0024	150.68 ± 4.5
6.	<i>A. pullulans</i> + 50% PVA	11.81 ± 0.065	0.08785 ± 0.0023	148.8 ± 8

Electrospun mat of pullulan without carrier polymer had contact angle of 57.5° indicating the hydrophilic nature of pullulan and, the electrospun mat of only PVA has the contact angle of 108.7° indicating the hydrophobic nature. The electrospun mats of blended polymers had contact angle of 101.3° for Commercial pullulan + 40% PVA, 110.4° for Commercial pullulan + 50% PVA, 98.0° for *A. pullulans* MTCC 1991 pullulan + 40% PVA, 104.7° for *A. pullulans* pullulan + 50% PVA.

In the DSC analysis, the electrospun pullulan mat without PVA did not show any endothermic peak around 220 °C, which is attributed to melting temperature of PVA (Fig. 8). This peak was prominent in all the electrospun blended mats of pullulan and PVA at around 220 °C.

As per the CIE colour space analysis, the lightness value, L\*, represents the darkest black at L\* = 0, and the brightest white at L\* = 100. The L\* (Lightness) values obtained for electrospun commercial pullulan was 91 whereas L\* values for electrospun pullulan extracted from, *A. pullulans* MTCC 1991 and *A. pullulans* were 91 and 90 respectively. When compared to standard white paper on which the electrospinning was carried out, ΔL\* values for electrospun, commercial pullulan, pullulan extracted from *A. pullulans* MTCC 1991 and *A. pullulans* were 2.408, 1.394 and 1.367, respectively. The redness/greenness color component, a\*, negative values indicate greenness while positive values indicate redness. The, a\*, values obtained for electrospun commercial pullulan was 2.126 whereas for electrospun pullulan extracted from, *A. pullulans* MTCC 1991 and *A. pullulans* were -0.006 and 1.090 respectively. The blueness/yellowness color component, b\*, negative values indicate blueness while positive values indicate yellowness. The, b\*, values obtained for electrospun commercial pullulan was -3.051 whereas for electrospun pullulan extracted from, *A. pullulans* MTCC 1991 and *A. pullulans* were 4.556 and 1.078 respectively. When the magnitude of the color difference, ΔE\*, is higher than 1, it indicates a visually detectable color difference and its value increases further for greater color changes. When compared to standard white paper on which the electrospinning was carried out, ΔE\* values for electrospun, commercial pullulan, pullulan extracted from *A. pullulans* MTCC 1991 and *A. pullulans* were 6.995, 16.219 and 12.873 respectively.

## Discussion:

Results of SEM and measurement of average diameter range of nanofibers indicated that the addition of PVA helps to reduce the diameter of nanofibres out of pullulan. Earlier work reported the diameter of composite pullulan-whey protein nanofibers made by electrospinning to be 231 nm (Drosou et al. 2018).

As per the results of AFM, the height and diameter of nanofibres increased by 40% and 70% for pullulan extracted from *A. pullulans* whereas it decreased by 40% and 35% for pullulan extracted from *A. pullulans* MTCC 1991, respectively, when compared to the nanofibres of commercial pullulan / PVA blend. The roughness of pullulan nanofibres increased by 45% and 10% for pullulans extracted from *A. pullulans* and filamentous yeast, respectively whereas it decreased by 35% for pullulan extracted from *A. pullulans* MTCC 1991 as compared to the commercial pullulan / PVA blend. In case of measurement of surface area, the difference in the extracted pullulan and commercial were less than 5%. Overall surface area calculated for all the samples were not significantly different.

As per the BET results in Table 7, the average pore radius electrospun nanofibres from pullulan of *A. pullulans* MTCC 1991 + 40% PVA was 80% more than its comparable commercial pullulan with 40% PVA. But, the average pore radius electrospun nanofibres from pullulan of *A. pullulans* + 50% PVA was 35% lesser than its comparable commercial pullulan with 50% PVA. The total pore volume of electrospun nanofibres from pullulan of *A. pullulans* + 50% PVA is 56% lesser than its comparable commercial pullulan with 50% PVA. On

the other hand, the total pore volume of electrospun nanofibres from pullulan of *A. pullulans* MTCC 1991 + 40% PVA was 14.5% more than its comparable commercial pullulan with 40% PVA. Thus, extracted pullulan gave better average pore radius and total pore volume as compared to commercial when same amount of PVA carrier polymer was added. The surface area of electrospun nanofibres from pullulan of *A. pullulans* MTCC 1991 + 40% PVA was 36.4% less than its comparable commercial pullulan with 40% PVA. The surface area of electrospun nanofibres from pullulan of *A. pullulans* + 50% PVA was 32% less than its comparable commercial pullulan with 50% PVA. This proves that finest nanofibres were produced from extracted pullulan from *A. pullulans* + 50% PVA. The surface area obtained in this work is very much higher than the reported value of 17.6 m<sup>2</sup>/g in case of electrospun gelatin nanofibres (Jakub et al. 2012) and 19.49 m<sup>2</sup>/g in case of  $\beta$ -Cyclodextrin based electrospun nanofibers (Zhao et al. 2015). Similar result was reported earlier wherein a facile route for fabrication of novel microporous material based on chitosan and PVA nanofibres resulted in high specific surface area (1680 m<sup>2</sup>/g), considerably small, pore volume (0.061 cc/g), and small pore radius (0.08 Å), as proved by BET analysis (Sargazi et al. 2018).

The wettability of a material surface is an important property that is described as the contact angle between the liquid and the material surface. It clearly showed that as the presence of PVA imparted hydrophobic effect to the electrospun pullulan mat. In all the cases, the contact angle of the blended polymer electrospun mat was in between that of pure pullulan and pure PVA. In an earlier report, the fluorinated silane functionalized superhydrophobic pullulan/poly(vinyl alcohol) blend membrane with water contact angle larger than 150° was prepared by the electrospinning method and characterized (Karim et al. 2011). Another study was reported earlier wherein the hydrophobicity was introduced in the biodegradable films using PVA (Karim et al. 2011; Dominguez-Martinez et al. 2017).

As per the DSC curves, the dramatic changes observed in the melting temperature of the blended mat can be attributed by the introduction of CF<sub>3</sub> groups into heteroatom (O atom) containing hydrophobic carbon ring of pullulan and hydrophobic carbon chain of PVA (Zalar et al. 2008; Liu et al. 2013; Karim et al. 2011).

As per the CIE colour space analysis, no significant difference in whiteness (L\*) was observed among various pullulan samples. The electrospun mat of extracted pullulan was darker than that of commercial pullulan as per the values of  $\Delta L^*$ . The commercial pullulan and one extracted from *A. pullulans* were found to be having redness color component whereas pullulan extracted from *A. pullulans* MTCC 1991 was found to be having greenness color component as per the values of a\*. The commercial pullulan was found to be having blueness color component whereas pullulan extracted from *A. pullulans* MTCC 1991 and *A. pullulans* MTCC 1991 were found to be having yellowness color component as per the values of b\*. According to the values of  $\Delta E^*$ , mat from electrospun extracted pullulan is having significant color difference than that of commercial pullulan.

## Conclusion

The isolate, *A. pullulans* yielded more pullulan (67.4 gL<sup>-1</sup>) as compared to *A. pullulans* MTCC 1991 (63.68 gL<sup>-1</sup>) in solid state fermentation. Wheat Bran, a low-cost and easily available waste material from wheat flour production, could provide an economic advantage as a solid substrate as well as sole carbon source for production of the pullulan by *A. pullulans* isolated from the *Peltophorum* species. Even though the specific surface area of the commercial pullulan was higher than the extracted pullulan nanofibres, the average pore size and total pore volume for extracted pullulan nanofibres were lesser than the commercial as calculated by BET analysis, indicating finer nanofibre formation. This in turn could be helpful for application based on retaining ability of the nanofibre mats at the nano level and thereby increasing the efficiency of the product. The pullulan extracted from *A. pullulans* MTCC 1991 as well as isolate, *A. pullulans* could be electrospun into nanofibres only when blended with PVA (40 -50%). The significant change in melting temperature of the blended electrospun mats as observed in DSC thermograms could be attributed to the addition of PVA. This work provides newer isolates for production of pullulan using wheat bran as carbon source and also the process protocol for production of nanofibre mat by electrospinning after blending with PVA.

## List Of Abbreviations

XRD X-ray diffractometer

BET Brunauer-Emmett-Teller

PVA poly (vinyl alcohol)

EPS exopolysaccharide

SF submerged fermentation

WB Wheat Bran

CSD Cotton Stalk Dust

SSF Solid State Fermentation

S.D. standard deviation

IPA Isopropyl alcohol

PEG 600 Polyethylene glycol 600

PDA Potato Dextrose Agar

YMA Yeast Morphology Agar

MEA Blakeslee's Malt Extract Agar

YNB Yeast Nitrogen Base

YCB Yeast Carbon Base

NCMR National Centre for Microbial Resource

APD automatic powder diffraction

FT-IR Fourier transform infrared

STP standard temperature and pressure

TCD tip to collector distance

SEM scanning electron microscope

AFM Atomic Force Microscope

CIE International Commission of Illumination

NFCCI National Fungal Culture Collection of India

ITS Internal transcribed spacer

TIFR Tata Institute for Fundamental Research

## **Declarations**

### **Ethics approval and consent to participate**

Not applicable.

### **Consent for publication**

Not applicable.

### **Availability of data and materials**

All data generated or analysed during this study are included in this published article.

### **Competing interests**

The authors declare that they have no competing interests.

## Funding

All the research work was funded by ICAR - Central Institute for Research on Cotton Technology, Matunga, Mumbai 400019, India.

## Authors' contributions

KS performed all the experimental methods and interpretation was carried out jointly by KS and NV.

## Acknowledgements

Authors acknowledge the support provided by Dr. P.G. Patil, Dr. S. Saxena, Dr. Charlene D' Souza, Dr. Nandita Ashtaputre, Mr. Nishant Kambli, Mr. Rajesh Kadam, Mr. Rajesh Narkar, Mr. G. B. Hadge and Mr. Prabhu Desai of ICAR-Central Institute for Research on Cotton Technology, Mumbai, India. Authors also acknowledge the support provided by the National Facility for High-field NMR, Tata Institute for Fundamental Research (TIFR), Colaba, Mumbai, India and National Fungal Culture Collection of India (NFCCI)-A National Facility, Agharkar Research Institute, Pune, India.

## References

1. Ray PC, Moorthy SN (2007) Exopolysachharide (pullulan) production from cassava starch residue by *Aureobasidium pullulans* strain MTCC 1991. *J Sci Ind Res (India)* 66:252-255
2. Singh RS, Saini GK, Kennedy JF (2008) Pullulan: Microbial sources, production and applications. *Carbohydr Polym* 73(4):515-531
3. Leathers TD (2003) Biotechnological production and applications of pullulan. *Appl Microbiol Biotechnol* 62(5):468-473
4. Knapp BK, Parsons CM, Bauer LL, Swanson KS, Fahey GC (2010) Soluble Fiber Dextrins and Pullulans Vary in Extent of Hydrolytic Digestion in Vitro and in Energy Value and Attenuate Glycemic and Insulinemic Responses in Dogs. *J Agric Food Chem* 58(21):11355-11363
5. Kong L, Ziegler GR (2014) Rheological aspects in fabricating pullulan fibers by electro-wet-spinning. *Food Hydrocoll* 38:220-226
6. Pollock TJ, Thorne L, Armentrout RW (1992) Isolation of new *aureobasidium* strains that produce high-molecular-weight pullulan with reduced pigmentation. *Appl Environ Microbiol* 58(3):877-883
7. Punnapayak H, Sudhadham M, Prasongsuk S, Pichayangkura S (2003) Characterization of *Aureobasidium pullulans* isolated from airborne spores in Thailand. *J Ind Microbiol Biotechnol* 30(2):89-94
8. Kang J-x, Chen X-j, Chen W-r, Li M-s, Fang Y, Li D-s, Ren Y-z, Liu D-q (2011) Enhanced production of pullulan in *Aureobasidium pullulans* by a new process of genome shuffling. *Process Biochem* 46(3):792-795
9. Prasongsuk S, Lotrakul P, Ali I, Bankeeree W, Punnapayak H (2018) The current status of *Aureobasidium pullulans* in biotechnology. *Folia Microbiol* 63(2):129-140
10. Urzi C, De Leo F, Lo Passo C, Criseo G (1999) Intra-specific diversity of *Aureobasidium pullulans* strains isolated from rocks and other habitats assessed by physiological methods and by random amplified polymorphic DNA (RAPD). *J Microbiol Methods* 36(1-2):95-105
11. Yurlova NA, Uijthof JMJ, de Hoog GS (1996) Distinction of species in *Aureobasidium* and related genera by PCR-ribotyping. *Antonie van Leeuwenhoek* 69(4):323
12. Zalar P, Gostincar C, de Hoog GS, Ursic V, Sudhadham M, Gunde-Cimerman N (2008) Redefinition of *Aureobasidium pullulans* and its varieties. *Stud Mycol* 61:21-38
13. Yurlova N, Hoog S, Gerrits van den Ende B (1999) Taxonomy of *Aureobasidium* and allied genera. *Stud Mycol* 43:63-69
14. Limtong S, Koowadjanakul N (2012) Yeasts from phylloplane and their capability to produce indole-3-acetic acid. *World J Microbiol Biotechnol* 28(12):3323-3335
15. Youssef F, Biliaderis CG, Roukas T (1998) Enhancement of pullulan production by *aureobasidium pullulans* in batch culture using olive oil and sucrose as carbon sources. *Appl Biochem Biotechnol* 74(1):13-30
16. Kim J-H, Kim M-R, Lee J-H, Lee J-W, Kim S-K (2000) Production of high molecular weight pullulan by *Aureobasidium pullulans* using glucosamine. *Biotechnol Lett* 22(12):987-990
17. Glushakova AM, Chernov IY (2010) Seasonal dynamics of the structure of epiphytic yeast communities. *Microbiology* 79(6):830-839
18. Sláviková E, Vadkertiová R, Vránová D (2009) Yeasts colonizing the leaves of fruit trees. *Ann Microbiol* 59(3):419-424

19. Landell MF, Billodre R, Ramos JP, Leoncini O, Vainstein MH, Valente P (2010) *Candida aechmeae* sp. nov. and *Candida vrieseae* sp. nov., novel yeast species isolated from the phylloplane of bromeliads in Southern Brazil. *Int J Syst Evol Microbiol* 60(Pt 1):244-248
20. Sharma RR, Singh D, Singh R (2009) Biological control of postharvest diseases of fruits and vegetables by microbial antagonists: A review. *Biol Control* 50(3):205-221. <https://doi.org/10.1016/j.biocontrol.2009.05.001>
21. Koowadjanakul N, Jindamorakot S, Yongmanitchai W, Limtong S (2011) *Ogataea phyllophila* sp. nov., *Candida chumphonensis* sp. nov. and *Candida matranensis* sp. nov., three methylotrophic yeast species from phylloplane in Thailand. *Antonie Van Leeuwenhoek* 100(2):207-217. <https://doi.org/10.1007/s10482-011-9579-9>
22. Kunkel ME, Seo A (1994) In Vitro digestibility of selected polymers. *J Environ Polym Degrad* 2(4):245-251. <https://doi.org/10.1007/BF02071972>
23. Liu Y, Wang R, Ma H, Hsiao BS, Chu B (2013) High-flux microfiltration filters based on electrospun polyvinylalcohol nanofibrous membranes. *Polymer* 54(2):548-556. <https://doi.org/10.1016/j.polymer.2012.11.064>
24. Eslamian M, Khorrami M, Yi N, Majd S, Abidian MR (2019) Electrospinning of highly aligned fibers for drug delivery applications. *J Mater Chem B* 7(2):224-232. <https://doi.org/10.1039/C8TB01258J>
25. Kurtzman CP, Fell JW, Boekhout T, Robert V (2011) Methods for Isolation, Phenotypic Characterization and Maintenance of Yeasts. In: Kurtzman CP, Fell JW, Boekhout T (eds) *The Yeasts* (Fifth Edition). Elsevier, London. <https://doi.org/10.1016/B978-0-444-52149-1.00007-0>
26. Choudhury AR, Bhattacharjee P, Prasad GS (2013) Development of Suitable Solvent System for Downstream Processing of Biopolymer Pullulan Using Response Surface Methodology. *PLOS ONE* 8(10):e77071. <https://doi.org/10.1371/journal.pone.0077071>
27. Karim MR, Islam MS (2011) Thermal Behavior with Mechanical Property of Fluorinated Silane Functionalized Superhydrophobic Pullulan/Poly(vinyl alcohol) Blends by Electrospinning Method. *J Nanomater* 2011:7. <https://doi.org/10.1155/2011/979458>
28. Sharmila G, Muthukumar C, Nayan G, Nidhi B (2013) Extracellular Biopolymer Production by *Aureobasidium pullulans* MTCC 2195 Using Jackfruit Seed Powder. *J Polym Environ* 21(2):487-494. <https://doi.org/10.1007/s10924-012-0459-9>
29. de Hoog GS, Yurlova NA (1994) Conidiogenesis, nutritional physiology and taxonomy of *Aureobasidium* and *Hormonema*. *Antonie van Leeuwenhoek* 65(1):41-54. <https://doi.org/10.1007/BF00878278>
30. Wu J, Zhong F, Li Y, Shoemaker CF, Xia W (2013) Preparation and characterization of pullulan–chitosan and pullulan–carboxymethyl chitosan blended films. *Food Hydrocoll* 30(1):82-91. <https://doi.org/10.1016/j.foodhyd.2012.04.002>
31. Xiao Q, Lu K, Tong Q, Liu C (2015) Barrier Properties and Microstructure of Pullulan–Alginate-Based Films. *J Food Process Eng* 38(2):155-161. <https://doi.org/10.1111/jfpe.12151>
32. Li R, Tomasula P, De Sousa AMM, Liu S-C, Tunick M, Liu K, Liu L (2017) Electrospinning Pullulan Fibers from Salt Solutions. *Polymers* 9(1):32
33. Arnosti C, Repeta DJ (1995) Nuclear Magnetic Resonance Spectroscopy of Pullulan and Isomaltose: Complete Assignment of Chemical Shifts. *Starch - Stärke* 47(2):73-75. <https://doi.org/10.1002/star.19950470208>
34. Ye L, Zhang J, Ye X, Tang Q, Liu Y, Gong C, Du X, Pan Y (2008) Structural elucidation of the polysaccharide moiety of a glycopeptide (GLPCW-II) from *Ganoderma lucidum* fruiting bodies. *Carbohydr Res* 343(4):746-752. <https://doi.org/10.1016/j.carres.2007.12.004>
35. Sugumaran KR, Jothi P, Ponnusami V (2014) Bioconversion of industrial solid waste–Cassava bagasse for pullulan production in solid state fermentation. *Carbohydr Polym* 99:22-30. <https://doi.org/10.1016/j.carbpol.2013.08.039>
36. Sugumaran KR, Sindhu RV, Sukanya S, Aiswarya N, Ponnusami V (2013) Statistical studies on high molecular weight pullulan production in solid state fermentation using jack fruit seed. *Carbohydr Polym* 98(1):854-860. <https://doi.org/10.1016/j.carbpol.2013.06.071>
37. Kim SE, Heo DN, Lee JB, Kim JR, Park SH, Jeon SH, Kwon IK (2009) Electrospun gelatin/polyurethane blended nanofibers for wound healing. *Biomed Mater* 4(4):044106. <https://doi.org/10.1088/1748-6041/4/4/044106>
38. Islam MS, Yeum JH, Das AK (2012) Effect of pullulan/poly(vinyl alcohol) blend system on the montmorillonite structure with property characterization of electrospun pullulan/poly(vinyl alcohol)/montmorillonite nanofibers. *J Colloid Interface Sci* 368(1):273-281. <https://doi.org/10.1016/j.jcis.2011.11.007>
39. Zhang Y, Huang X, Duan B, Wu L, Li S, Yuan X (2007) Preparation of electrospun chitosan/poly(vinyl alcohol) membranes. *Colloid Polym Sci* 285(8):855-863. <https://doi.org/10.1007/s00396-006-1630-4>
40. Drosou C, Krokida M, Biliaderis CG (2018) Composite pullulan-whey protein nanofibers made by electrospinning: Impact of process parameters on fiber morphology and physical properties. *Food Hydrocoll* 77:726-735. <https://doi.org/10.1016/j.foodhyd.2017.11.014>



41. Jakub S, Hobzov R, Kostina N, Munzarov M, Jukl M, Lhotka M, Kubinov S, Alena Z, Jiri M (2012) Morphological Characterization of Nanofibers: Methods and Application in Practice. *J Nanomater* 2012:14. <https://doi.org/10.1155/2012/327369>
42. Zhao R, Wang Y, Li X, Sun B, Wang C (2015) Synthesis of  $\beta$ -Cyclodextrin-Based Electrospun Nanofiber Membranes for Highly Efficient Adsorption and Separation of Methylene Blue. *ACS Appl Mater Inter* 7(48):26649-26657. <https://doi.org/10.1021/acsami.5b08403>
43. Sargazi G, Afzali D, Mostafavi A, Ebrahimipour SY (2018) Synthesis of CS/PVA Biodegradable Composite Nanofibers as a Microporous Material with Well Controllable Procedure Through Electrospinning. *J Polym Environ* 26(5):1804-1817. <https://doi.org/10.1007/s10924-017-1080-8>
44. Dominguez-Martinez BM, Martínez-Flores HE, Berrios JDJ, Otoni CG, Wood DF, Velazquez G (2017) Physical Characterization of Biodegradable Films Based on Chitosan, Polyvinyl Alcohol and Opuntia Mucilage. *J Polym Environ* 25(3):683-691. <https://doi.org/10.1007/s10924-016-0851-y>

## Figures

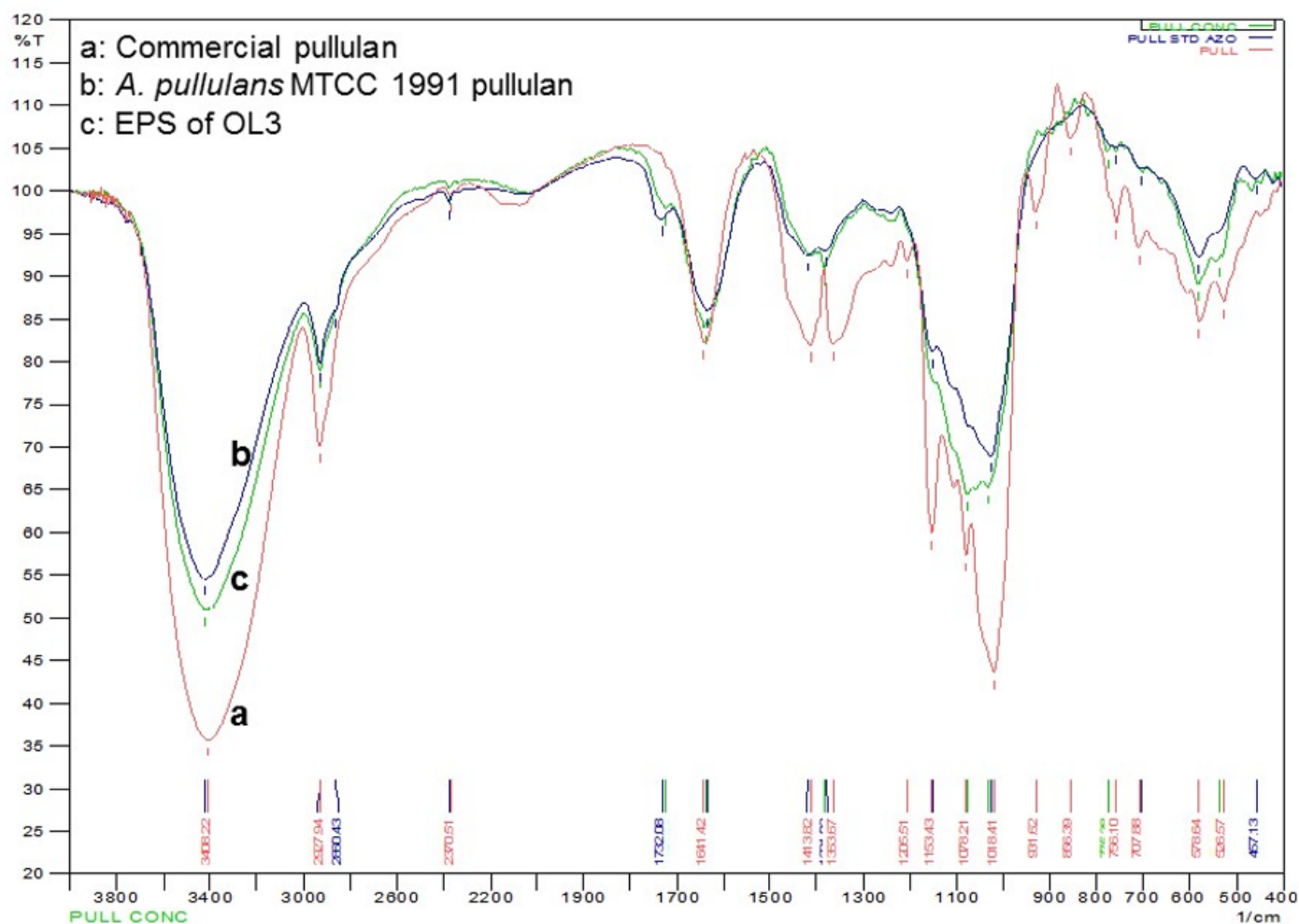


**Figure 1**

FTIR spectra of Commercial Pullulan (a), Pullulan of *A. pullulans* MTCC 1991 (b) and EPS of OL3 (c)

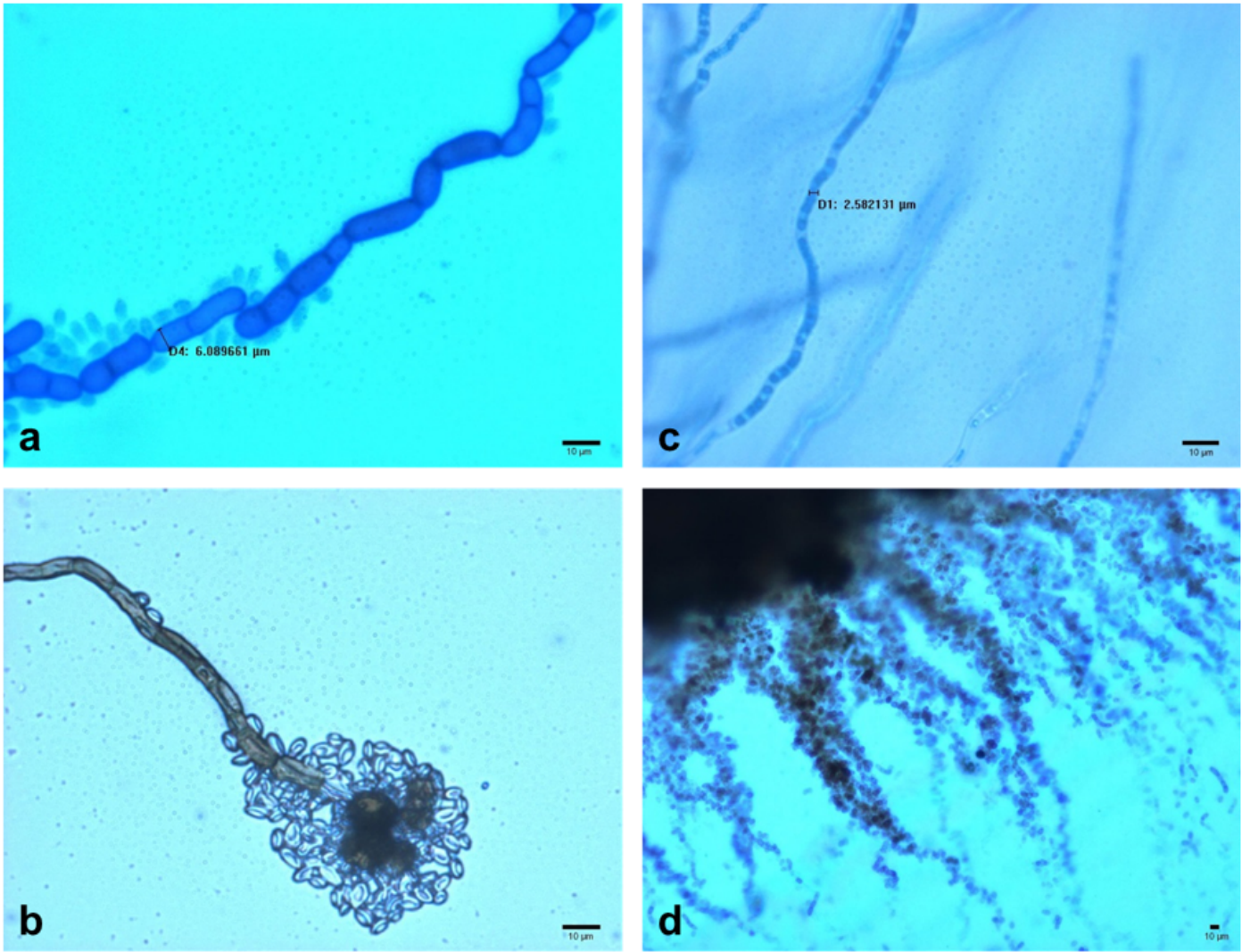


**Figure 2**

Microscopic images of *A. pullulans* MTCC 1991 showing septate hyphae diameter of 6.08 μm (a), conidiospore bearing conidia of *A. pullulans* MTCC 1991 observed at 400x magnification (b), Isolate OL3 showing septate hyphae diameter of 2.34 μm (c) and protunicate asci and blastic conidiogenesis of OL3 observed at 100x magnification (d)

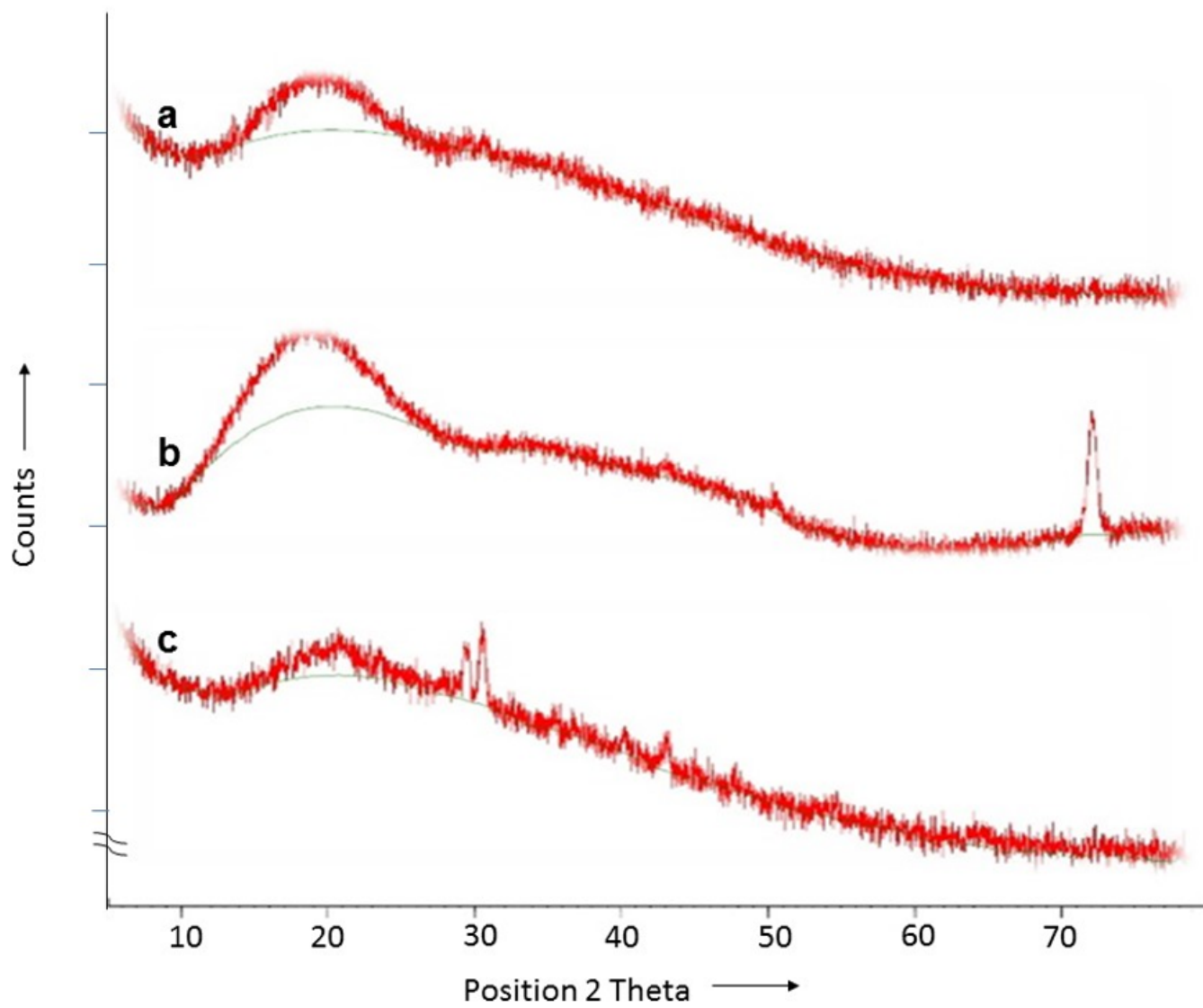


**Figure 3**

XRD spectra of extracted pullulan from commercial pullulan (a), *A. pullulans* MTCC 1991 (b) and *A. pullulans* (c)

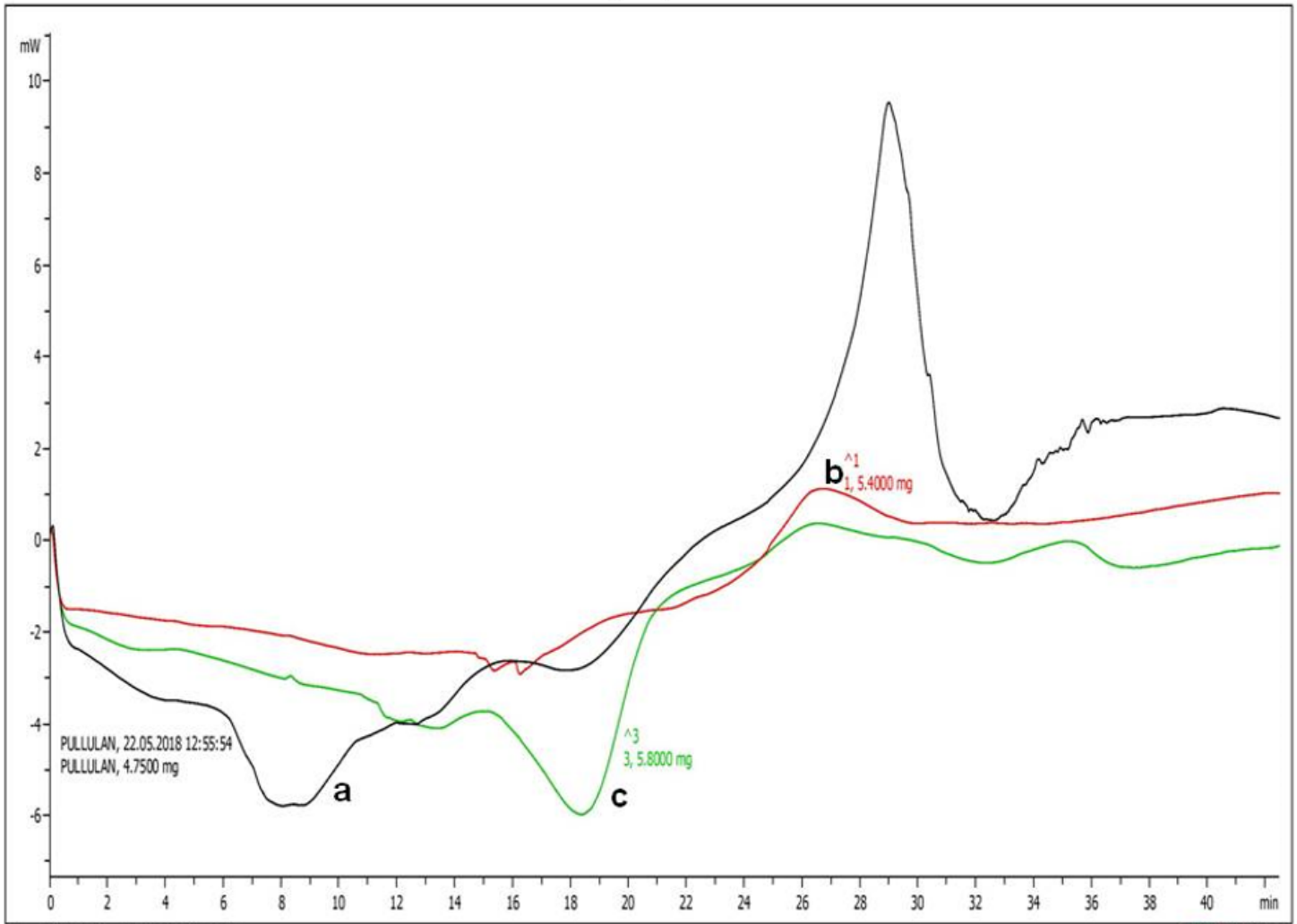


**Figure 4**

DSC thermograms of Commercial Pullulan (Black) (a), Pullulan of *A. pullulans* MTCC 1991 (Red) (b) and Pullulan of *A. pullulans* (Green) (c)

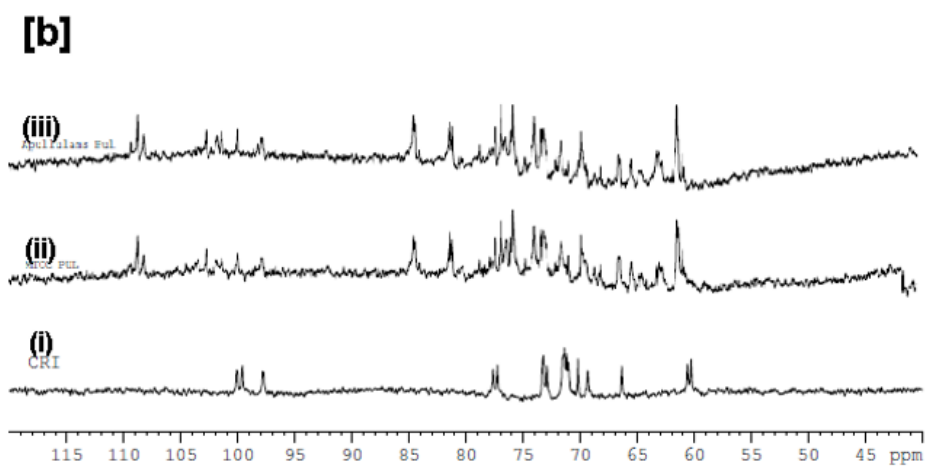
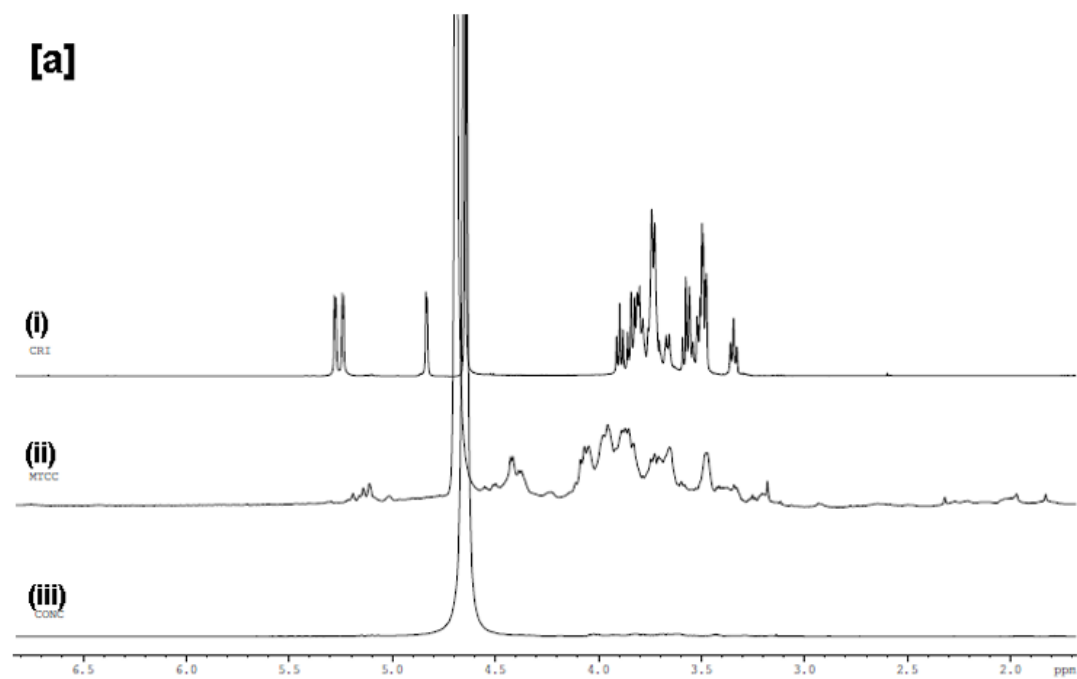


**Figure 5**

$^1\text{H}$ -NMR spectra [a] of commercial pullulan (i) and extracted pullulan from *A. pullulans* MTCC 1991 (ii) and *A. pullulans* (iii);  $^{13}\text{C}$ -NMR spectra [b] of commercial pullulan (i) and extracted pullulan from *A. pullulans* MTCC 1991 (ii) and *A. pullulans* (iii)

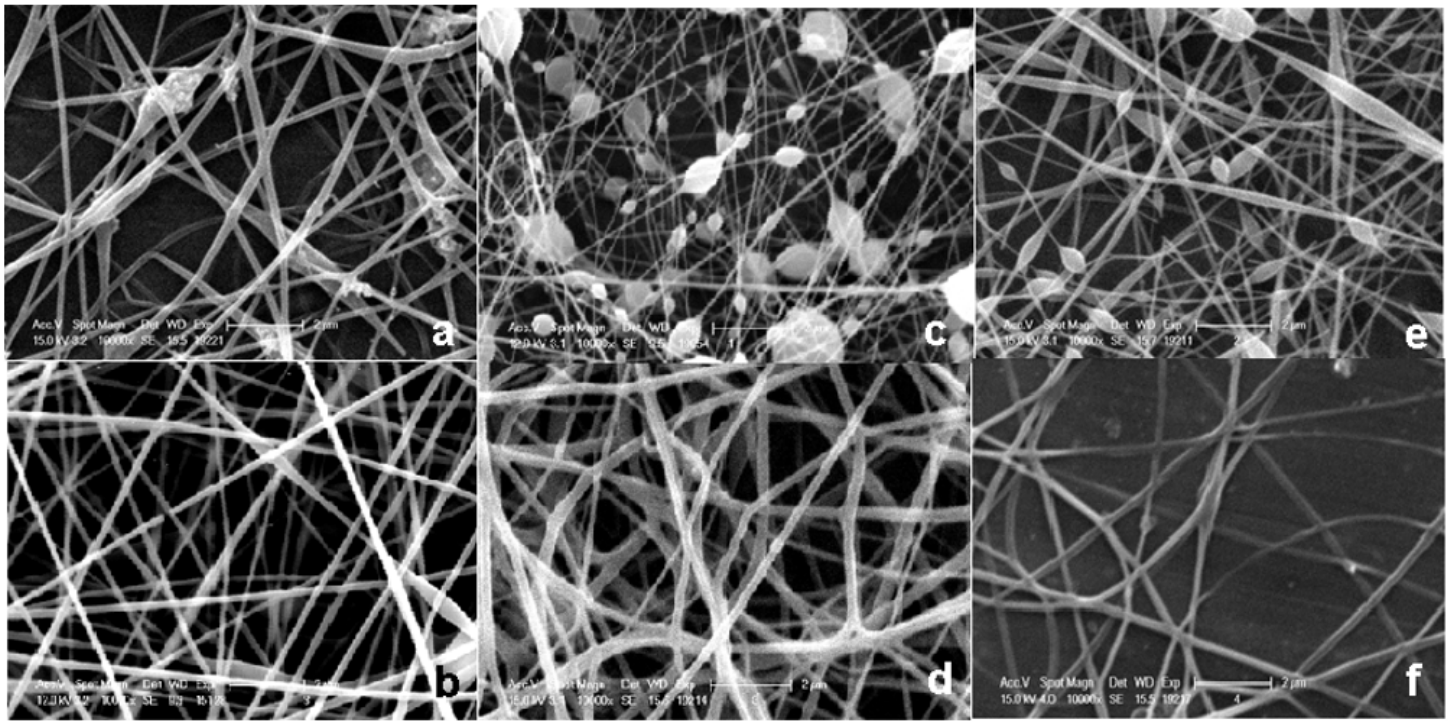


Figure 6

SEM images of electrospun nanofibers of Commercial pullulan (a); Commercial PVA (b); Commercial pullulan with 40% Poly vinyl alcohol (PVA) (c); Pullulan extracted from *A. pullulans* MTCC 1991 with 40% PVA (d); Commercial pullulan with 50% PVA (e) and Pullulan extracted from *A. pullulans* with 50% PVA (f). All images have been taken at 10,000x magnification and scale bars in images represent 2 μm

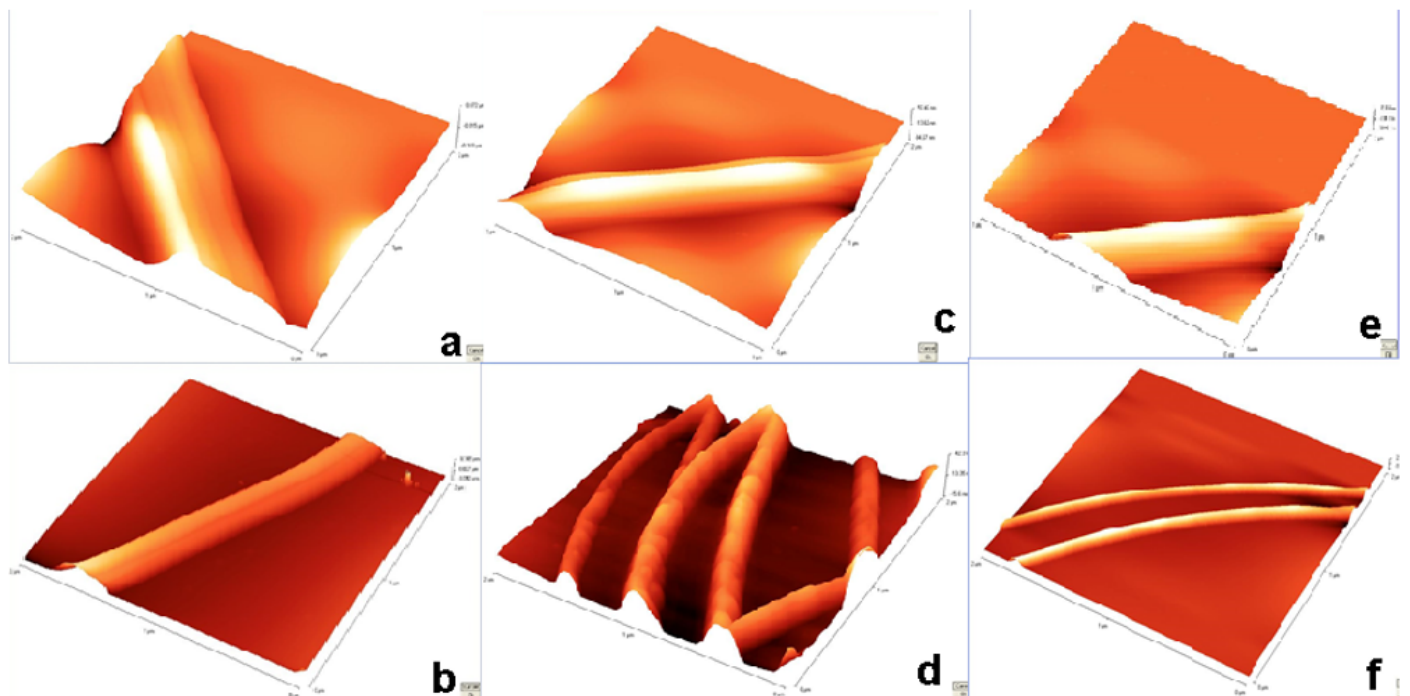
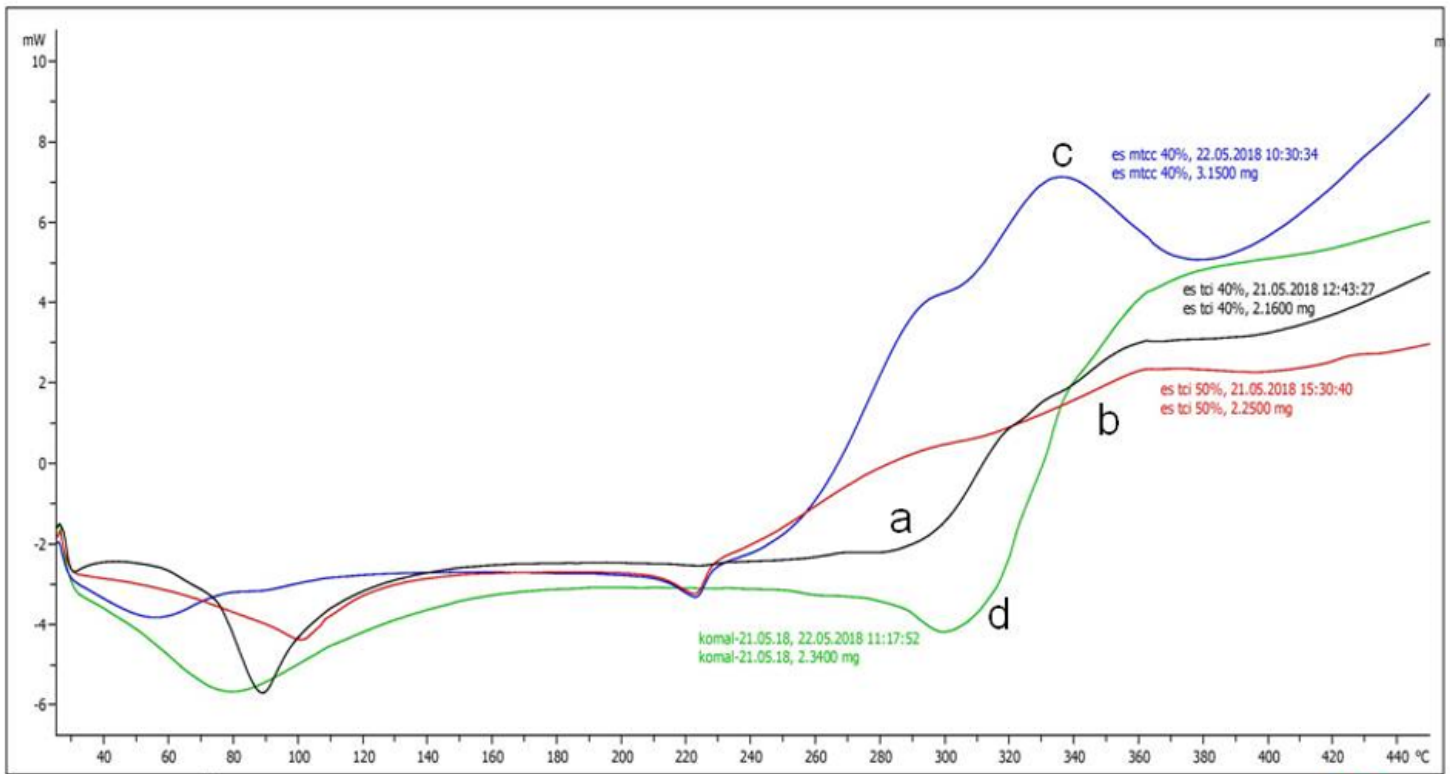


Figure 7

AFM 3D images of electrospun nanofibres of Commercial pullulan (a); Commercial PVA (b); Commercial pullulan with 40% Poly vinyl alcohol (PVA) (c); Pullulan extracted from *A. pullulans* MTCC 1991 with 40% PVA (d); Commercial pullulan with 50% PVA (e) and Pullulan extracted from *A. pullulans* with 50% PVA (f) at the scale of 2 $\mu$ m



**Figure 8**

DSC thermogram of electrospun nanofibre mats of commercial pullulan with 40% PVA (a), commercial pullulan with 50% PVA (b), pullulan extracted from *A. pullulans* MTCC 1991 + 40% PVA (c) and pullulan extracted from *A. pullulans* + 50% PVA (d)

## Supplementary Files

This is a list of supplementary files associated with this preprint. Click to download.

- [Graphicalabstract.jpg](#)